# Organization of cytoplasmic domains of sarcoplasmic reticulum Ca$^{2+}$-ATPase in E$_1$P and E$_1$ATP states: a limited proteolysis study

Stefania Danko[a], Kazuo Yamasaki[a], Takashi Daiho[a], Hiroshi Suzuki[a,*], Chikashi Toyoshima[b]

[a]*Department of Biochemistry, Asahikawa Medical College, Midorigaokahigashi, Asahikawa 078-8510, Japan*
[b]*Institute of Molecular and Cellular Biosciences, The University of Tokyo, Bunkyo-ku, Tokyo 113-0032, Japan*

**Abstract** In order to characterize the domain organization of sarcoplasmic reticulum Ca$^{2+}$-ATPase in different physiological states, limited proteolysis using three proteases (proteinase K (prtK), V8 and trypsin) was conducted systematically and quantitatively. The differences between E$_2$ and E$_2$P were examined in our previous study and E$_2$P was characterized by the complete resistance to all three proteases (except for trypsin attack at the very top of the molecule (T1 site)). The same strategies were employed in this study for E$_1$ATP, E$_1$PADP and E$_1$P states. Because of the transient nature of these states, they were either stabilized by non-hydrolyzable analogues or made predominant by adjusting buffer conditions. Aluminum fluoride (without ADP) was found to stabilize E$_1$P. All these states were characterized by strong (E$_1$ATP) to complete (E$_1$PADP and E$_1$P) resistance to prtK and to V8 but only weak resistance to trypsin at the T2 site. Because prtK and V8 primarily attack the loops connecting the A domain to the transmembrane helices whereas the trypsin T2 site (Arg$^{198}$) is located on the outermost loop in the A domain, these results lead us to propose that the A domain undergoes a large amount of rotation between E$_1$P and E$_2$P. Combined with previous results, we demonstrated that four states can be clearly distinguished by the susceptibility to three proteases, which will be very useful for establishing the conditions for structural studies. © 2001 Federation of European Biochemical Societies. Published by Elsevier Science B.V. All rights reserved.

*Key words:* Ca$^{2+}$-ATPase; P-type ion transporting ATPase; Ca$^{2+}$ pump; Sarcoplasmic reticulum; Phosphorylated intermediate; Proteolysis

## 1. Introduction

Sarcoplasmic reticulum (SR) Ca$^{2+}$-ATPase is a 110 kDa membrane protein and a representative member of P-type ion transporting ATPases. It catalyzes Ca$^{2+}$ transport coupled with ATP hydrolysis [1,2]. According to the E$_1$/E$_2$ theory, the enzyme with bound Ca$^{2+}$ (E$_1$) is autophosphorylated by ATP bound at the catalytic site to form ADP-sensitive phosphoenzyme (E$_1$P). This phosphorylation causes the bound Ca$^{2+}$ ions

to be occluded at the transport sites, and the subsequent conformational transition to the ADP-insensitive form (E$_2$P) releases Ca$^{2+}$ into the lumen. Finally, dephosphorylation takes place and returns the enzyme into the unphosphorylated and Ca$^{2+}$-unbound E$_2$ form (for recent reviews, see [3,4]).

Ca$^{2+}$-ATPase has three cytoplasmic domains (A, N and P), which are widely separated in the crystal structure with bound Ca$^{2+}$ ([5], CaE$_1$ in Fig. 1). It has been proposed that when Ca$^{2+}$ is absent, three cytoplasmic domains gather to form a single headpiece. This was based on the modeling of the enzyme in tubular crystals formed in the presence of decavanadate and in the absence of Ca$^{2+}$ ([5], E$_2$V in Fig. 1). Then, an obvious and important issue to be addressed now is in which steps in the catalytic cycle such large domain movements take place. We would like to know if the movement of A domain is co-ordinated with the movement of N domain, and if the binding of ATP itself affects the domain organization. To answer these questions we believe that, although very classic, limited proteolysis is useful, because these proteases cleave quite distinct sites (Fig. 1). Proteinase K (prtK) cleaves primarily the loops connecting A domain to M2 and M3 transmembrane helices [6], V8 the loop connecting A domain to M3 helix [7]; trypsin attacks the outermost loop of A domain (T2 site) in addition to the loop at the top of N domain (T1 site) [8]. We first studied the difference between E$_2$ and E$_2$P [10] and demonstrated that E$_2$P is characterized by the complete resistance to all the three proteases (except for trypsin attack at T1 site). Because of the same resistance properties, the enzyme in the tubular crystals (E$_2$V) was identified to be in a state very close to E$_2$P. These results provided a strong support for the proposal that A domain rotates a large amount, because the protection of T2 site by P domain requires a nearly 90° rotation of A domain.

We now extend the same strategies to E$_1$ATP complex and E$_1$P to complete the characterization by limited proteolysis of various states in the catalytic cycle. The design of the experiments is as follows. Although it is impossible to stop the reaction in E$_1$ATP state, we could use non-hydrolyzable analogues (adenosine 5′-(β,γ-methylene)triphosphate (AMPPCP) in this study) to mimic E$_1$ATP; the effect of γ-phosphate can be addressed by comparing with ADP. 2′,3′-$O$-(2,4,6-Trinitrocyclohexadienylidene) (TNP)-AMP and TNP-ATP may also be useful for deciphering the effects of different parts of ATP. The E$_1$PADP state can be made with Al$^{3+}$/F$^-$/ADP [11]. We also show that Al$^{3+}$/F$^-$ alone (without ADP) stabilizes E$_1$P. The E$_1$P to E$_2$P transition can be blocked partially by adding a high concentration of Ca$^{2+}$ or completely by using $N$-ethylmaleimide (NEM)-treated specimen [12]. We report here that

*Corresponding author. Fax: (81)-166-68 2359.
E-mail address:* hisuzuki@asahikawa-med.ac.jp (H. Suzuki).

$E_1P$ and $E_1ATP$ have similar patterns of susceptibility, but distinctly different from those examined previously, including $E_2P$ [10]. Taken altogether, we can now distinguish four states unequivocally by limited proteolysis. The results also indicate that the large rotation of A domain will take place between $E_1P$ and $E_2P$.

## 2. Materials and methods

### 2.1. Preparation of SR vesicles and treatment with NEM

SR vesicles were prepared from rabbit skeletal muscle as described previously [13]. The content of phosphorylation site determined with $^{32}P_i$ according to Barrabin et al. [14] was $5.0 \pm 0.2$ nmol/mg of vesicle protein ($n = 6$). The $Ca^{2+}$-dependent ATPase activity determined at 25°C as described previously [13] was $2.51 \pm 0.05$ μmol/min/mg of vesicle protein ($n = 3$). SR vesicles were treated with NEM in the presence of adenosine $5'$-($\beta,\gamma$-imido)triphosphate (AMPPNP) according to Kawakita et al. [12]. The content of phosphorylation site was unaffected and the $Ca^{2+}$-dependent ATPase activity was completely suppressed by this treatment due to blocking of the $E_1P$ to $E_2P$ transition [12,15]. The NEM-treated vesicles were used in some proteolysis experiments with ATP.

### 2.2. Proteolysis of SR vesicles

SR vesicles (0.3 mg/ml of vesicle protein) were digested with prtK, V8 protease, or trypsin in a buffer containing 0.1 M KCl, 7 mM $MgCl_2$, 0.5 mM $CaCl_2$ plus 0.4 mM EGTA (0.103 mM $Ca^{2+}$ at pH 6.7) or 20 mM $CaCl_2$ without EGTA, and 50 mM 3-(N-morpholino)-propanesulfonic acid/Tris (pH 6.7) or 50 mM 2-(N-morpholino)ethanesulfonic acid/Tris (pH 6.0), as stated in the legends for figures and tables. The concentration (mg/ml) of the protease and temperature were 0.05 (pH 6.7) or 0.1 (pH 6.0) and 25°C for the prtK proteolysis, 0.065 (pH 6.7 and pH 6.0) and 37°C for the V8 proteolysis, and 0.03 (pH 6.7) or 0.1 (pH 6.0) and 25°C for the tryptic proteolysis, respectively. For the V8 proteolysis, octaethylene glycol monododecyl ether at a non-solubilizing low concentration of 0.05 mg/ml was included in the reaction mixture as described previously [7]. Effects of ATP and its analogues were examined with ATP ($\pm 5$ mM), AMPPCP ($\pm 1$ mM), ADP ($\pm 100$ μM), TNP-AMP ($\pm 10$ μM) and TNP-ATP ($\pm 10$ μM),

unless otherwise stated. ATP was added 5 s before the start of the proteolysis, and other nucleotides 5 min before the start. When the effects of $Al^{3+}/F^-/ADP/Mg^{2+}$ were examined, SR vesicles were pre-incubated essentially according to Troullier et al. [11] with $AlCl_3$ ($\pm 50$ μM), KF ($\pm 3$ mM), ADP ($\pm 100$ μM) and $MgCl_2$ ($\pm 7$ mM) for 40 min at 22°C and pH 6.7 in the presence of 0.1 mM $Ca^{2+}$, and then the proteolysis was started.

Proteolysis was terminated by adding ice-cold trichloroacetic acid to 2.5% (w/v) and diluting three times with a modified Laemmli sample buffer containing 3% (w/v) sodium dodecyl sulfate (SDS). 20 μl of each sample thus obtained was loaded on a 10.5% gel for SDS–poly-acrylamide gel electrophoresis according to Laemmli [16]. For better resolution of the peptides on SDS gels, 1 mM $CaCl_2$ was included in both the stacking and separating gels for the V8- and prtK-treated samples [7]. The gels were stained by Coomassie brilliant blue R-250, and subjected to densitometric analysis with a GT9500-GT95FLU flatbed scanner (Epson, Tokyo, Japan) and Scion Image software (Scion Corp., Frederick, MD, USA).

### 2.3. Miscellaneous methods

V8 protease, prtK, trypsin (L-1-tosylamido-2-phenylethyl chloromethyl ketone-treated) were obtained from Sigma. AMPPCP and AMPPNP were also from Sigma. TNP-AMP and TNP-ATP were synthesized according to Hiratsuka [17]. Protein concentrations were determined by the method of Lowry et al. [18] with bovine serum albumin as a standard. Data were analyzed by non-linear regression using the program Origin (Microcal Software, Inc., Northampton, MA, USA).

## 3. Results

### 3.1. Degradation of SR $Ca^{2+}$-ATPase by proteases

Proteolysis of SR $Ca^{2+}$-ATPase in the presence of $Ca^{2+}$ was carried out using prtK, V8 protease and trypsin to examine the effects of ATP, AMPPCP, ADP, TNP-AMP, TNP-ATP, $Al^{3+}$, $F^-$ and $Mg^{2+}$. Typical digestion patterns with prtK and trypsin are shown in Fig. 2. The degradation of the 110 kDa ATPase chain with prtK measured by densitometric scan of the SDS gels was well approximated by first order reaction
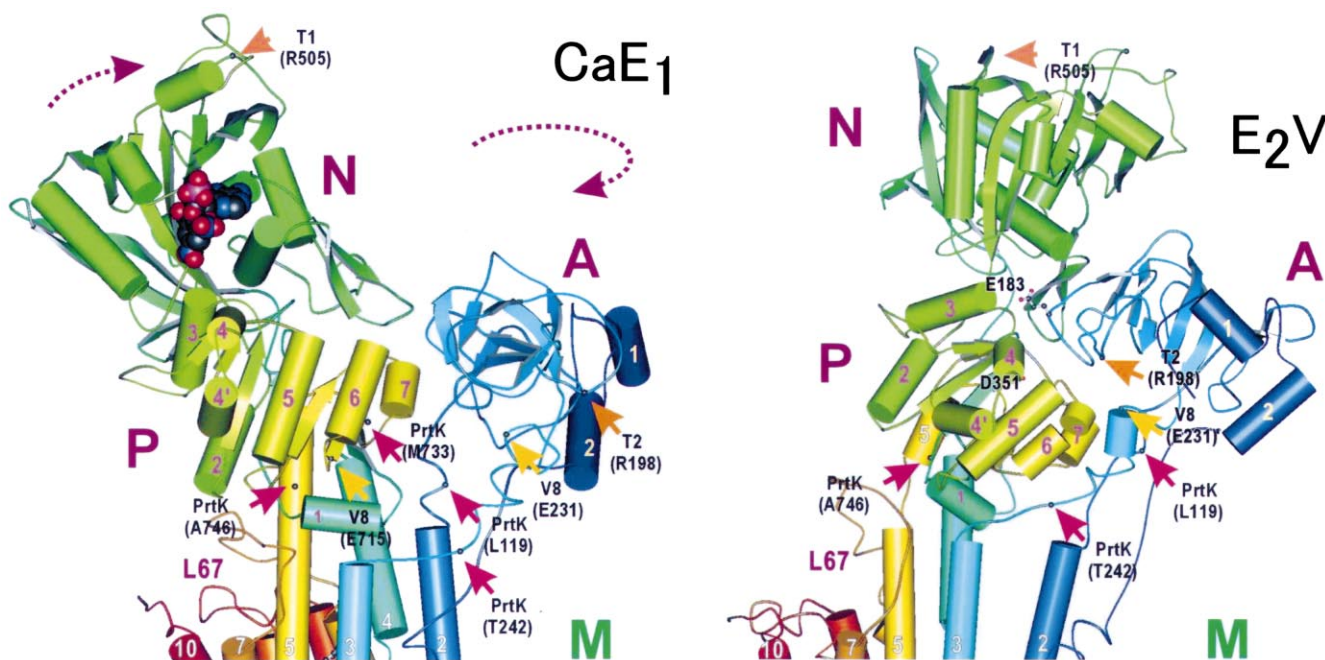


Fig. 1. Location of proteolytic cleavage sites on SR $Ca^{2+}$-ATPase. The positions of the main digestion sites by prtK [6], V8 [7] and trypsin [8] are shown on the atomic model of $Ca^{2+}$-ATPase [5] with bound $Ca^{2+}$ ($CaE_1$; PDB accession code 1EUL) and that made for the decavanadate-bound form in the absence of $Ca^{2+}$ ($E_2V$; PDB accession code 1FQU), which is analogous to $E_2P$ [10]. The arrows in broken lines show the movements of A and N domains required to fit the atomic model of the $Ca^{2+}$-bound state ($CaE_1$) to that of $E_2V$.

Table 1
Effects of AMPPCP, ADP, TNP-AMP and TNP-ATP on the degradation rate of SR $Ca^{2+}$-ATPase

| Protease | Relative rate constant (%) | | | | |
|---|---|---|---|---|---|
| | No ligands | AMPPCP | ADP | TNP-AMP | TNP-ATP |
| PrtK | 100 | 15 (36) | 100 | 70 | 70 |
| V8 protease | 100 | 9 (7) | 90 | 102 | 104 |
| Trypsin (T2) | 100 | 63 (89) | 85 | 79 | 128 |

SR vesicles were digested with prtK, V8 and trypsin at pH 6.7 in the presence of $Ca^{2+}$ (0.1 mM), $Mg^{2+}$ (7 mM) and nucleotides, as described in Section 2. The rate constants given are those for the degradation of the 110 kDa $Ca^{2+}$-ATPase polypeptide chain (prtK and V8) and those for the formation of A1 fragment (trypsin, cleavage at $Arg^{198}$ (T2)). The numbers were obtained by least-squares fit as described in Fig. 2 and given in percentages to those obtained in the absence of nucleotides (no ligands). The numbers in parentheses show the rates in the presence of AMPPCP but in the absence of $Mg^{2+}$; they were normalized to the rates in the absence of both AMPPCP and $Mg^{2+}$ (100%). The results obtained with AMPPCP at 3 mM, ADP at 0.5 mM, and TNP-AMP and TNP-ATP at 30 (and 3) μM (data not shown) were almost the same as those listed above obtained with AMPPCP at 1 mM, ADP at 0.1 mM, and TNP-AMP and TNP-ATP at 10 μM, respectively.

kinetics (Fig. 2A,C). In all the trypsin digestion experiments, the cleavage at T1 site ($Arg^{505}$) was very rapid and produced A and B fragments. The formation of the C-terminal A1 fragment upon further cleavage of A fragment at the T2 site ($Arg^{198}$) and its subsequent degradation were well described by consecutive first order reaction kinetics (Fig. 2B,D). All the major digestion products by prtK, V8 and trypsin were found to be consistent with those published previously [6–9,19–22]. Only the relative rate constants for the degradation of 110 kDa ATPase chain (prtK and V8 proteolysis) and those for the formation of A1 fragment (trypsin proteolysis) are therefore listed in Tables 1–3. Table 1 summarizes the effects of nucleotide binding. The numbers for stable $E_1P$ analogues are given in Table 2. Table 3 summarizes the experiments with ATP.

### 3.2. Effects of nucleotides on digestion of SR $Ca^{2+}$-ATPase

The effects of nucleotide binding to $Ca^{2+}$-ATPase in the presence of 0.1 mM $Ca^{2+}$ and 7 mM $MgCl_2$ were examined with AMPPCP, ADP, TNP-AMP and TNP-ATP (Table 1). AMPPCP, a non-hydrolyzable ATP analogue that will fix the enzyme in the $E_1ATP$ state [13,23–25], was clearly different from others. Only AMPPCP provided strong resistance against prtK and V8, and protected A1, A2 and B tryptic fragments from further degradation. TNP-ATP did not show such protection effects. On the other hand, none of the nucleotides provided strong resistance to trypsin cleavage at the T2 site, although AMPPCP somewhat slowed down the degradation process. TNP-ATP even accelerated the degradation. Thus the γ-phosphate was essential for these protections but the TNP moiety impaired them.

### 3.3. Effects of $Al^{3+}$, $F^-$, ADP and $Mg^{2+}$ on digestion of SR $Ca^{2+}$-ATPase

Aluminum fluorides ($AlF_3$ and $AlF_4^-$) have been used widely as γ-phosphate analogues for ATPases and GTPases

[11,26–29]. With $Ca^{2+}$-ATPase, Troullier et al. [11] demonstrated that $AlF_4^-$ and ADP make a stable complex with the enzyme in the presence of $Ca^{2+}$ and $Mg^{2+}$, presumably fixing the enzyme in $E_1PADP$, the state immediately after phosphorylation with ATP. Digestion experiments with this complex showed complete resistance to prtK and to V8, but only a weak resistance to trypsin (Table 2). We then examined the protection effects for all the possible combinations of the four components (i.e. $Al^{3+}$, $F^-$, ADP, $Mg^{2+}$), and found that $Al^{3+}/F^-/ADP$ (no $Mg^{2+}$) and $Al^{3+}/F^-/Mg^{2+}$ were also equally effective. Hence we consider that the complex of $Ca^{2+}$-ATPase with $Al^{3+}/F^-/ADP$ represents $E_1PADP$ whereas $Al^{3+}/F^-/Mg^{2+}$ represents $E_1P$ and that they have similar compact domain organizations. Judging from the digestion rates of the 110 kDa ATPase chain and those at the tryptic T2 site, the domain organizations in $E_1PADP$ and $E_1P$ are close to that in $E_1ATP$, but distinctly different from that in $E_2P$ (completely resistant to trypsin attack at the T2 site [10]).

### 3.4. Effects of ATP on digestion of SR $Ca^{2+}$-ATPase

To make the enzyme predominantly in the $E_1P$ state with the natural substrate (ATP), we tried two ways. The first was to add 20 mm $Ca^{2+}$ (in the presence of $K^+$) so that the transition from $E_1P$ to $E_2P$ is largely blocked; low pH (pH 6) was chosen to avoid too rapid exhaustion of ATP. As expected, nearly complete protection was found against prtK and V8 (Table 3). The second was to use NEM-treated specimen with which the $E_1P$ to $E_2P$ transition is completely blocked [12,15]. With this specimen, complete protection against prtK and V8 was observed even at pH 6.7 and low $Ca^{2+}$ concentration (0.1 mM).

## 4. Discussion

As described, $E_1ATP$, $E_1PADP$ and $E_1P$ states of SR $Ca^{2+}$-ATPase can now be characterized by a strong resistance to

Table 2
Effects of $Al^{3+}$, $F^-$ and ADP on the degradation rate of SR $Ca^{2+}$-ATPase

| Protease | Relative rate constant (%) | | | | | | | |
|---|---|---|---|---|---|---|---|---|
| | No ligands | $Al^{3+}/F^-/ADP$ | $Al^{3+}/F^-$ | $Al^{3+}/ADP$ | $ADP/F^-$ | $F^-$ | $Al^{3+}$ | ADP |
| PrtK | 100 | 2, 0 (1) | 8 (56) | 93 | 60 | 101 | 111 | 100 |
| V8 protease | 100 | 0 (0) | 0 (83) | 101 | 70 | 50 | 108 | 90 |
| Trypsin (T2) | 100 | 71 (76) | 64 (125) | 100 | 68 | 87 | 93 | 85 |

SR vesicles were treated with the ligands ($Al^{3+}$, $F^-$ and ADP) at pH 6.7 in the presence of $Ca^{2+}$ (0.1 mM) and $Mg^{2+}$ (7 mM), and then digested with prtK, V8 and trypsin, as described in Section 2. Refer to Table 1 for the meaning of the 'relative rate constant'. The numbers in parentheses show the degradation rates in the presence of the ligands but in the absence of $Mg^{2+}$; they were normalized to the rates in the absence of both the ligands and $Mg^{2+}$ (100%).
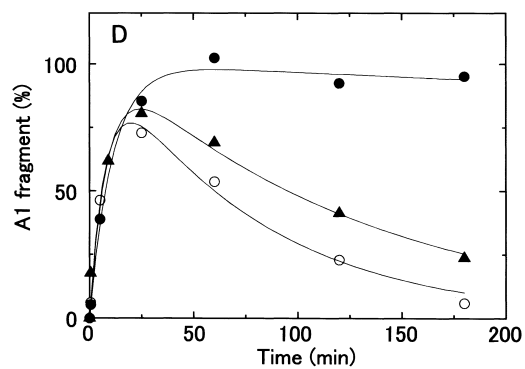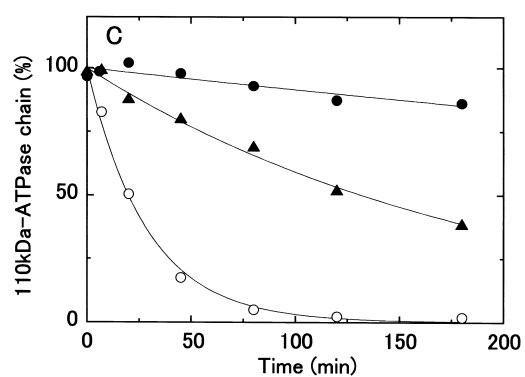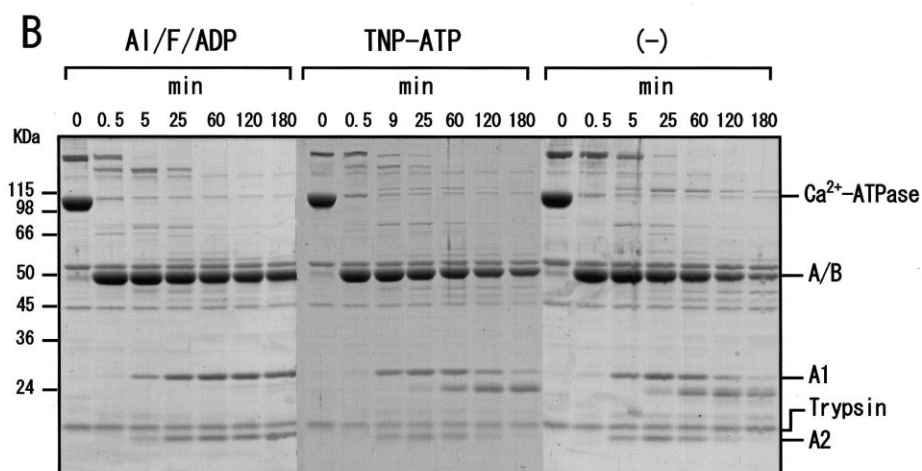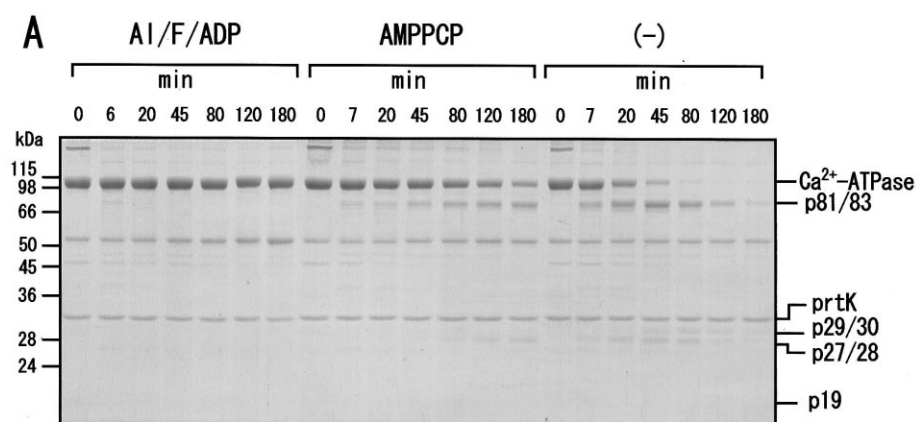
Fig. 2. Effects of AMPPCP, TNP-ATP and $Al^{3+}/F^-/ADP$ on the prtK and trypsin digestion of SR $Ca^{2+}$-ATPase. SR vesicles treated with $Al^{3+}$, $F^-$ and ADP (Al/F/ADP), and untreated vesicles preincubated with AMPPCP (AMPPCP) and TNP-ATP (TNP-ATP) or without those ligands (−), were digested with prtK (A, C) and trypsin (B, D) in the presence of 7 mM $Mg^{2+}$ and 0.1 mm $Ca^{2+}$ at pH 6.7, as described in Section 2. A: SDS gels of the prtK digests, and (B) those of the trypsin digests. The positions of $Ca^{2+}$-ATPase and its proteolytic fragments, and those of the molecular mass markers are indicated on the right and the left margins, respectively. C: The time courses for the amounts of the 110 kDa $Ca^{2+}$-ATPase polypeptide chain in prtK digestion with the $Al^{3+}/F^-/ADP$-treated (●) and untreated (○, ▲) vesicles in the absence (○) or presence (▲) of AMPPCP. D: The time courses for the amounts of A1 fragment in trypsin digestion with the $Al^{3+}/F^-/ADP$-treated (●) and untreated (○, ▲) vesicles in the absence (○) or presence (▲) of TNP-ATP. Solid lines in (C) show least-squares fit of a single exponential to the time course for the amounts of the 110 kDa ATPase chain, in which the first order rate constants ($h^{-1}$) were 0.053 for the $Al^{3+}/F^-/ADP$-treated vesicles, 2.1 for the untreated vesicles, and 0.32 for the untreated vesicles in the presence of AMPPCP. Solid lines in (D) show least-squares fit of a double exponential in a consecutive formation and decay reaction to the time course for the amounts of A1 fragment, in which the formation rate constants and decay rate constants ($h^{-1}$) were 5.5 and 0.022 for the $Al^{3+}/F^-/ADP$-treated vesicles, 7.7 and 0.80 for the untreated vesicles, and 7.1 and 0.48 for the untreated vesicles in the presence of TNP-ATP.

←

prtK and to V8 but a weak resistance to trypsin at the T2 site. This is in marked contrast with $E_2P$, which is characterized by complete resistance to all of these [10]. The protection against prtK and V8 was somewhat less in $E_1ATP$ stabilized by AMPPCP than in $E_1P$. This difference will probably be explained by the equilibrium between $E_1$ and $E_1AMPPCP$, considering that digestion proceeds irreversibly if the population of enzyme in $E_1$ state exists at all. Thus, combined with our previous results [10], four states in the reaction cycle ($E_1$, $E_1ATP$ or $E_1P$, $E_2P$ and $E_2$) can be distinguished by their characteristic differences in the susceptibilities to three proteases, which can be quantitated simply by relative digestion rates (Table 4).

Then the question is how these proteolysis results can be interpreted in the light of three-dimensional (3D) structure. Can we consider in a simple minded way that the decreases in degradation rate constants represent the steric blocks of the cleavage sites? Of course we cannot exclude the possibility that conformational changes unrelated to domain movements altered the susceptibility of the cleavage sites. However, 3D structure modeled for vanadate-induced tubular crystals ([5], $E_2V$ in Fig. 1; analogous to $E_2P$) and that determined for $Mg^{2+}/F^-$ complex (a stable $E_2P$ analogue [30–33]; Toyoshima et al., unpublished results) showed that all the cleavage sites are blocked sterically by gathering of all three cytoplasmic domains. Hence in the following discussion, we simply relate the protection effects with steric blocking due to domain movements schematized in Fig. 3.

The simplest interpretation of the observed protections in $E_1ATP$ and $E_1P$ is that N and P domains are in closed configuration crosslinked by ATP (having adenosine on one end and γ-phosphate on the other end), by $Al^{3+}/F^-/ADP$ or $Al^{3+}/F^-/Mg^{2+}$ (presumably due to strong interaction of fluoride with amide nitrogen), or by phosphate covalently bound to $Asp^{351}$. Absolute requirement of γ-phosphate for the protec-

tion was evident, because ADP showed no effect for the primary cleavage site ($Glu^{243}$) (Table 1). Also reported was a protection by AMPPNP, another non-hydrolyzable ATP analogue, of A1 and A2 tryptic fragments from further degradation [20]. Bidentate β,γ-CrATP, which stabilizes the $Ca^{2+}$-occluded state (analogous to $E_1P$) [34], conferred resistance to prtK [35] but not to trypsin [21]. It is understandable that the TNP moiety impaired the protection effects, because TNP-ATP is virtually non-hydrolyzable with $Ca^{2+}$-ATPase [36,37]. Presumably, the TNP moiety, which provides much higher affinity for TNP-ATP than ATP [38,39], prevents proper binding of the ATP moiety to the enzyme and positioning of γ-phosphate.

Because the adenosine moiety of ATP is considered to bind around $Phe^{487}$ in N domain and because the phosphorylation site ($Asp^{351}$) on P domain is distant by ~25 Å in the crystal structure of the $Ca^{2+}$-bound ($E_1$) state [5], very large motion of domain closure is necessary for the γ-phosphate to reach the phosphorylation site. In the model for the vanadate-induced tubular crystals ($E_2V$ in Fig. 1; analogous to $E_2P$), N domain is closer to P domain by ~20° compared to that in the $E_1$ state; this amount is still too small for bringing the γ-phosphate to $Asp^{351}$. This is also true for glutaraldehyde crosslinking, which is most reactive in $E_1P$ but unreactive in $E_2P$, between $Lys^{492}$ in N domain and $Arg^{678}$ in P domain [40]. Therefore, in the $E_1ATP$ and in $E_1P$ form, N domain may come even closer to P domain than in the $E_2V$ ($E_2P$) form (Fig. 3).

Then, it is likely that, in $E_1ATP$ and $E_1P$, A domain does not come to the position in which A and N domains can make several hydrogen bonds to stabilize the interaction between them as in $E_2P$. This view is totally consistent with the observation that the T2 site on A domain is rapidly cleaved in $E_1ATP$ and $E_1P$, but completely resistant in $E_2P$. Therefore, a large motion of A domain, i.e. rotation by ~90°, and its strong association with P and N domains occur most likely during the $E_1P$ to $E_2P$ transition (Fig. 3).

The large motion of domain closure of N and P domains in $E_1ATP$ and $E_1P$ will inevitably cause distortion in P domain, at least in the half closer to N domain. In fact, fluorescence from EDANS attached to $Cys^{674}$ in that half of P domain changes greatly on the formation of $E_1ATP$ (and only slightly by going further into $E_1P$) [23–25,41]. The distortion will likely cause the movement of M3 and the loop connecting A domain (possibly through the hydrogen bond between $Glu^{340}$ on Pα1 and $Thr^{247}$ (see figure 8 in [5]), or through the interaction with the loop connecting M6 and M7 because the mutations there slow down the phosphorylation [42]).

Then, 'in $E_1ATP$ and $E_1P$, does A domain occupy a posi-

Table 3
Effects of ATP on the degradation rate of SR $Ca^{2+}$-ATPase

| Protease | Relative rate constant (%) | | |
|---|---|---|---|
| | No ATP | Native SR | NEM-modified SR |
| PrtK | 100 | 5 (22) | 0 (1) |
| V8 protease | 100 | 2 | $0^a$ ($12^a$) |
| Trypsin (T2) | 100 | 68 | ND |

Effects of ATP on prtK, V8 and trypsin digestion of the unmodified (native SR) and NEM-modified (NEM-modified SR) $Ca^{2+}$-ATPases were examined at pH 6.0 in the presence of 20 mm $CaCl_2$, or 0.5 mm $CaCl_2$ plus 0.4 mm EGTA (the numbers in parentheses), as described in Section 2. Refer to Table 1 for the meaning of the 'relative rate constant'. ND: not determined.
[a]Determined at pH 6.7.

Table 4
Relative digestion rates for the intermediates in the catalytic cycle of SR $Ca^{2+}$-ATPase

| Protease | Primary cleavage sites | Relative rate constant (%) | | | | | | |
|---|---|---|---|---|---|---|---|---|
| | | $E_2^b$ (no ligands) | $E_1^{a,b}$ ($Ca^{2+}$) | $E_1ATP^a$ (AMPPCP) | $E_1PADP^a$ ($Al^{3+}/F^-/ADP$) | $E_1P^a$ ($Al^{3+}/F^-/Mg^{2+}$, ATP) | $E_2P^b$ ($Mg^{2+}/F^-$, orthovanadate) | $E_2V^b$ (decavanadate) |
| PrtK | L119($\downarrow$), T242($\uparrow$), M733/A746 | 100 | 113 | 17 | 0 | 0 | 1 | 0 |
| V8 protease | E231($\uparrow$), E715($\downarrow$) | 100 | 107 | 10 | 0 | 0 | 0 | 0 |
| Trypsin (T2) | R198($\uparrow$) | 100 | 211 | 133 | 150 | 135 | 0 | 0 |

The representative numbers for digestion rates obtained in our present and previous [10] studies for the six major intermediates ($E_2$, $E_1$, $E_1ATP$, $E_1PADP$, $E_1P$, and $E_2P$) in the catalytic cycle of $Ca^{2+}$-ATPase were summarized together with those for the decavanadate-bound state without $Ca^{2+}$ ($E_2V$), which forms the tubular crystals [46]. The ligands used for stabilizing individual states are shown in parentheses. In the prtK and V8 digestion, the rate constants for the degradation of the 110 kDa $Ca^{2+}$-ATPase polypeptide chain were shown. In the trypsin digestion, the rate constants for the cleavage at $Arg^{198}$ (T2) were shown. The rate constants were normalized to that obtained in the absence of $Ca^{2+}$ and ligands ($E_2$ (no ligands)) (100%). The primary cleavage sites [6–8] were listed with their C-terminal residues: ($\uparrow$) and ($\downarrow$) indicate the increase and decrease, respectively, in the cleavage rate of the $Ca^{2+}$-bound state ($E_1$) compared to the unbound state ($E_2$).
[a]Data obtained in this study.
[b]Data obtained in our previous study [10].

tion different from that in $E_1$?' will be the next question. Probably so. The protection against trypsin attack in $E_1ATP$ and $E_1P$ states was far from complete (only to 2/3 in the rate constant) but significant. The complete protection against prtK in these states will imply that the loop connecting M3 and A domain has moved toward and is protected by P domain (Fig. 1). The complete protection against V8 means that the part (around $Glu^{231}$) of the same loop closer to A domain has also moved and that the part of P domain (including $Glu^{715}$) that makes contacts with the upper part of M3 has become inaccessible to the protease. Therefore, it is likely that, in $E_1ATP$ and $E_1P$, A domain has moved toward P domain, but the domain is not yet rotated as in $E_2P$ (Fig. 3).

These notions on the domain arrangements are in complete agreement with the results by Fe-catalyzed cleavage of $Na^+,K^+$-ATPase. Karlish and co-workers proposed using this technique [43] that A domain is not in close contact with P domain in $E_1ATP$ and $E_1P$, but is so in $E_2P$. They showed that TGES sequence (starting from $Thr^{181}$ with $Ca^{2+}$-ATPase) comes close to TGDGVND (starting from $Thr^{701}$ with $Ca^{2+}$-ATPase) in $E_2P$. The location of T2 site ($Arg^{198}$) is very close to $Glu^{183}$ in the 3D structure (Fig. 1; [5]).

All these data support the idea that cytoplasmic domains of $Ca^{2+}$-ATPase take distinctly different arrangements in the catalytic cycle, and show that they can be distinguished by limited proteolysis. The results also strongly suggest that the
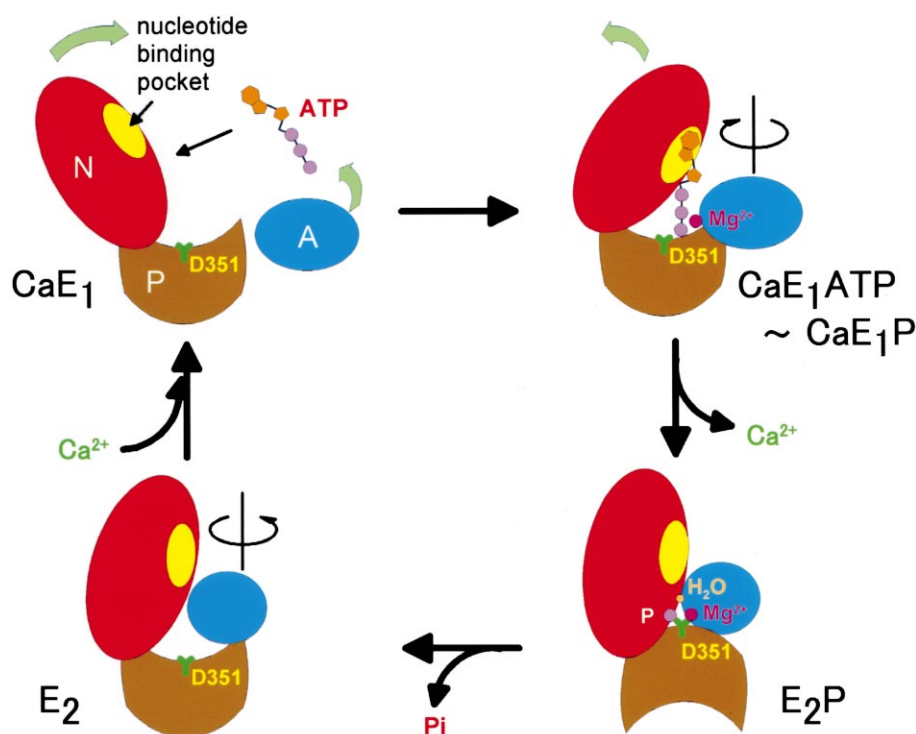


Fig. 3. Schematic models for four distinct arrangements of three cytoplasmic domains (N, P and A) in the catalytic cycle of $Ca^{2+}$-ATPase. Arrows indicate the proposed domain movements. In the text and tables, 'CaE$_1$' and 'CaE$_1$ATP' to 'CaE$_1$P' were described without 'Ca' for simplicity.

large rotation of A domain takes place during the $E_1P$ to $E_2P$ transition and this rearrangement is likely to be a key event in the whole reaction cycle. In fact, the enzyme cleaved at $Glu^{231}$ by V8 can be phosphorylated by ATP but does not undergo normal enzymatic turnover (due to blocking of the $E_1P$ to $E_2P$ transition) [7]. This is also the case with the enzyme cleaved at $Thr^{242}$ by prtK [9]. In the enzyme cleaved at T3b site ($Lys^{234}$ or $Arg^{236}$) by trypsin, the $E_1P$ to $E_2P$ transition is blocked [22]. Mutations of $Gly^{233}$, which is highly conserved among P-type ATPases, result in a very slow transition of $E_1P$ to $E_2P$ [44]. Furthermore, glutaraldehyde-crosslinked enzyme, presumably fixed in an $E_1ATP$-like configuration, does not proceed from $E_1P$ to $E_2P$ [40]. All these data suggest that $Ca^{2+}$-ATPase utilizes A domain for realizing the hydrophobic atmosphere [45] around the phosphorylation site in $E_2P$ state so that a specific water molecule can attack the acylphosphate (Fig. 3). Also the stabilization energy provided by intimate contacts between all three cytoplasmic domains in $E_2P$ will provide energy for moving transmembrane helices and release bound $Ca^{2+}$ ions.

Finally, for structural studies of intermediate states, it is vital to find conditions to stabilize them perfectly and efficient methods for examining how stable they are. The methods and conditions established in this (for $E_1P$) and our previous (for $E_2P$) [10] studies must be useful for making good crystals.

## References

[1] Ebashi, S. and Lipmann, F. (1962) J. Cell Biol. 14, 389–400.

[2] Hasselbach, W. and Makinose, M. (1961) Biochem. Z. 333, 518–528.

[3] MacLennan, D.H., Rice, W.J. and Green, N.M. (1997) J. Biol. Chem. 272, 28815–28818.

[4] Møller, J.V., Juul, B. and le Maire, M. (1996) Biochim. Biophys. Acta 1286, 1–51.

[5] Toyoshima, C., Nakasako, M., Nomura, H. and Ogawa, H. (2000) Nature 405, 647–655.

[6] Juul, B., Turc, H., Durand, M.L., Gomez de Gracia, A., Denoroy, L., Møller, J.V., Champeil, P. and le Maire, M. (1995) J. Biol. Chem. 270, 20123–20134.

[7] le Maire, M., Lund, S., Viel, A., Champeil, P. and Moller, J.V. (1990) J. Biol. Chem. 265, 1111–1123.

[8] Brandl, C.J., Green, N.M., Korczak, B. and MacLennan, D.H. (1986) Cell 44, 597–607.

[9] Juul, B. and Møller, J.V. (2000) in: Na/K-ATPase and Related ATPases (Taniguchi, K. and Kaya, S., Eds.), pp. 233–236, Elsevier, Amsterdam.

[10] Danko, S., Daiho, T., Yamasaki, Y., Kamidochi, M., Suzuki, H. and Toyoshima, C. (2001) FEBS Lett. 489, 277–282.

[11] Troullier, A., Girardet, J.-L. and Dupont, Y. (1992) J. Biol. Chem. 267, 22821–22829.

[12] Kawakita, M., Yasuoka, K. and Kaziro, Y. (1980) J. Biochem. (Tokyo) 87, 609–617.

[13] Nakamura, S., Suzuki, H. and Kanazawa, T. (1994) J. Biol. Chem. 269, 16015–16019.

[14] Barrabin, H., Scofano, H.M. and Inesi, G. (1984) Biochemistry 23, 1542–1548.

[15] Suzuki, H. and Kanazawa, T. (1995) J. Biol. Chem. 270, 3089–3093.

[16] Laemmli, U.K. (1970) Nature 227, 680–685.

[17] Hiratsuka, T. (1982) Biochim. Biophys. Acta 719, 509–517.

[18] Lowry, O.H., Rosebrough, N.J., Farr, A.L. and Randall, R.J. (1951) J. Biol. Chem. 193, 265–275.

[19] Dux, L. and Martonosi, A. (1983) J. Biol. Chem. 258, 10111–10115.

[20] Imamura, Y., Saito, K. and Kawakita, M. (1984) J. Biochem. (Tokyo) 95, 1305–1313.

[21] Andersen, J.P., Vilsen, B., Collins, J.H. and Jørgensen, P.L. (1986) J. Membr. Biol. 93, 85–92.

[22] Imamura, Y. and Kawakita, M. (1989) J. Biochem. (Tokyo) 105, 775–781.

[23] Kubo, K., Suzuki, H. and Kanazawa, T. (1990) Biochim. Biophys. Acta 1040, 251–259.

[24] Suzuki, H., Nakamura, S. and Kanazawa, T. (1994) Biochemistry 33, 8240–8246.

[25] Kanazawa, T., Suzuki, H., Daiho, T. and Yamasaki, K. (1995) Biosci. Rep. 15, 317–326.

[26] Coleman, D.E., Berghuis, A.M., Lee, E., Linder, M.E., Gilman, A.G. and Sprang, S.R. (1994) Science 265, 1405–1412.

[27] Sondek, J., Lambright, D.G., Noel, J.P., Hamm, H.E. and Sigler, P.B. (1994) Nature 372, 276–279.

[28] Fisher, A.J., Smith, C.A., Thoden, J.B., Smith, R., Sutoh, K., Holden, H.M. and Rayment, I. (1995) Biochemistry 34, 8960–8972.

[29] Braig, K., Menz, R.I., Montgomery, M.G., Leslie, A.G.W. and Walker, J.E. (2000) Structure 8, 567–573.

[30] Murphy, A.J. and Coll, R.J. (1992) J. Biol. Chem. 267, 5229–5235.

[31] Murphy, A.J. and Coll, R.J. (1992) J. Biol. Chem. 267, 16990–16994.

[32] Kubota, T., Daiho, T. and Kanazawa, T. (1993) Biochim. Biophys. Acta 1163, 131–143.

[33] Daiho, T., Kubota, T. and Kanazawa, T. (1993) Biochemistry 32, 10021–10026.

[34] Vilsen, B. and Andersen, J.P. (1992) J. Biol. Chem. 267, 3539–3550.

[35] Møller, J.V., Ning, G., Maunsbach, A.B., Fujimoto, K., Asai, K., Juul, B., Lee, Y.-J., Gomez de Gracia, A., Falson, P. and le Maire, M. (1997) J. Biol. Chem. 272, 29015–29032.

[36] Watanabe, T. and Inesi, G. (1982) J. Biol. Chem. 257, 11510–11516.

[37] Dupont, Y., Pougeois, R., Ronjat, M. and Verjovsky-Almeida, S. (1985) J. Biol. Chem. 260, 7241–7249.

[38] Dupont, Y., Chapron, Y. and Pougeois, R. (1982) Biochem. Biophys. Res. Commun. 106, 1272–1279.

[39] Suzuki, H., Kubota, T., Kubo, K. and Kanazawa, T. (1990) Biochemistry 29, 7040–7045.

[40] McIntosh, D.B. (1992) J. Biol. Chem. 267, 22328–22335.

[41] Suzuki, H., Obara, M., Kubo, K. and Kanazawa, T. (1989) J. Biol. Chem. 264, 920–927.

[42] Zhang, Z., Lewis, D., Sumbilla, C., Inesi, G. and Toyoshima, C. (2001) J. Biol. Chem. 276, 15232–15239.

[43] Patchornik, G., Goldshleger, R. and Karlish, S.J.D. (2000) Proc. Natl. Acad. Sci. USA 97, 11954–11959.

[44] Andersen, J.P., Vilsen, B., Leberer, E. and MacLennan, D.H. (1989) J. Biol. Chem. 264, 21018–21023.

[45] de Meis, L., Martins, O.B. and Alves, E.W. (1980) Biochemistry 19, 4252–4261.

[46] Dux, L. and Martonosi, A. (1983) J. Biol. Chem. 258, 2599–2603.